

FYS4560 - Elementary Particle Physics

---

## PROJECT 2

---

Jon Vegard Sparre

March 10, 2017

## Abstract

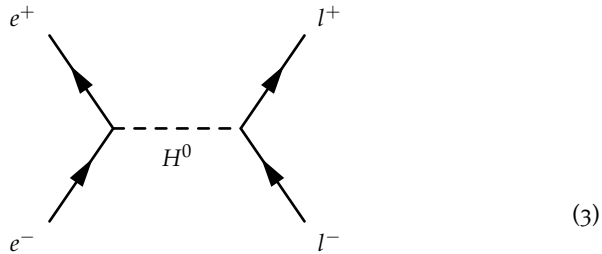
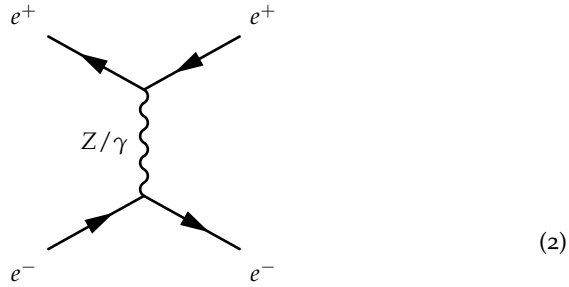
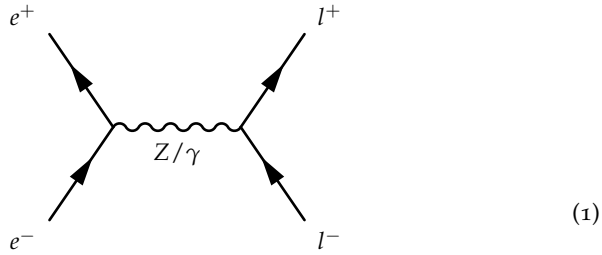
In this project we'll look at di-lepton production in the Standard Model by calculating the QED and electroweak cross section for muon pair production. We'll also discuss the various lepton pair production cases, electroweak asymmetry and compare our results to CompHEP.

In part II we look at physics beyond the SM with the  $Z'$  boson and slepton pair production as examples. Experimental limits and CompHEP calculations for  $Z'$  are discussed. For slepton pair production we'll look at competing SM background and how to detect it experimentally.

Detailed calculations and computer code used is available here: <https://github.com/jonvegards/FYS4560/tree/master/project2>

# 1 Di-lepton production in $e^+e^-$ in the SM

## 1.1 Feynman graphs



In fig. (1) we see the s-channel Feynman diagram for  $e^+e^-$  annihilating into a  $Z$  or a  $\gamma$  which decays into a lepton pair. This diagram contributes at all energies, with a peak at the  $Z$ -mass. The diagram in fig. (2) contributes only for  $e^+e^-$

into  $e^+e^-$ . The last diagram, fig. (3) is the smallest contributing diagram. The Higgs-coupling are proportional to the fermion's mass and since we are looking at electrons this coupling is extremely small so we don't need to take this into our calculations.

We have tree possible lepton pairs that we can get out of the reaction, electrons, muons and tau. The electrons are stable particles and will set off all it's energy in the e.m. calorimeter in the detector and is thus easy to detect. The muons will go out of the detector, but leave a trace in the muon chambers. The tau particles is a bit more cumbersome because of their large mass, according to PDG only 36% of the taus decays into electrons or muons, so we can expect many events with hadron jets.

## 1.2 QED calculation

Detailed calculation may be found in appendix A. We start by finding the amplitude for the QED reaction by looking at the Feynman graph:

$$i\mathcal{M} = \bar{v}^{s'}(p')(-ie\gamma^\mu)u^s(p)\left(\frac{-ig_{\mu\nu}}{q^2}\right)\bar{u}^r(k)(-ie\gamma^\nu)v^{r'}(k').$$

This we will square and put into,

$$\frac{d\sigma}{d\Omega} = \frac{1}{2E_{\text{CM}}} \frac{|\vec{k}|}{16\pi^2 E_{\text{CM}}} \frac{1}{4} \sum_{s,s',r,r'} |\mathcal{M}|^2.$$

The squared amplitude is,

$$|\mathcal{M}|^2 = \frac{e^4}{q^4} (\bar{v}(p')\gamma^\mu u(p)\bar{u}(p)\gamma^\nu v(p)) (\bar{u}(k)\gamma_\mu v(k')\bar{v}(k')\gamma_\nu u(k)).$$

Spin sums are here implicit. Since we want a cross section for an unpolarized electron-positron beam we'll sum over spins and get,

$$\frac{1}{4} \sum_{s,s',r,r'} |\mathcal{M}|^2 = \frac{1}{4} \frac{e^4}{q^4} \text{tr}((\not{p}' - m_e)\gamma^\mu(\not{p} + m_e)\gamma^\nu) \text{tr}((\not{k} + m_\mu)\gamma_\mu(\not{k}' - m_\mu)\gamma_\nu),$$

where we have used,

$$\sum_s u^s(p)\bar{u}^s(p) = \not{p} + m \quad \sum_s v^s(p)\bar{v}^s(p) = \not{p} - m.$$

The traces above can be somewhat simplified,

$$\frac{1}{4} \sum_{s,s',r,r'} |\mathcal{M}|^2 = \frac{8e^4}{q^4} \left( (p' \cdot k)(p \cdot k') + (p \cdot k)(p' \cdot k') + (p' \cdot p)m_\mu^2 \right),$$

where we on the way also ignored the electron masse since the muon mass is much larger. To get a more readable expression for the cross section, we can do some kinematics. We have,

$$\begin{aligned} q^2 &= (p + p')^2 = 4E^2, \\ p \cdot p' &= 2E^2, \\ p \cdot k &= p' \cdot k' = E^2 - E|\vec{k}|\cos\theta, \\ p \cdot k' &= p' \cdot k = E^2 + E|\vec{k}|\cos\theta, \\ |\vec{k}| &= \sqrt{E^2 - m_\mu^2} \sim E, \end{aligned}$$

which gives us

$$\begin{aligned} \frac{1}{4} \sum_{s,s',r,r'} |\mathcal{M}|^2 &= \frac{8e^4}{q^4} \left( (E^2 + E|\vec{k}| \cos \theta)^2 + (E^2 + E|\vec{k}| \cos \theta)^2 + 2E^2 m_\mu^2 \right) \\ &= e^4 \left( \left( 1 + \frac{m_\mu^2}{E^2} \right) + \left( 1 - \frac{m_\mu^2}{E^2} \right) \cos^2 \theta \right). \end{aligned}$$

Inserting this into the expression for the differential cross section, we get,

$$\left( \frac{d\sigma}{d\Omega} \right)_{\text{CM}} = \frac{1}{2E_{\text{CM}}} \frac{E}{16\pi^2 E_{\text{CM}}} e^4 \left( \left( 1 + \frac{m_\mu^2}{E^2} \right) + \left( 1 - \frac{m_\mu^2}{E^2} \right) \cos^2 \theta \right),$$

integrating this over  $d\Omega$  gives us,

$$\begin{aligned} \sigma_{\text{CM}} &= \frac{4\pi\alpha^2}{3E_{\text{CM}}^2} \sqrt{1 - \frac{m_\mu^2}{E^2}} \left( 1 + \frac{1}{2} \frac{m_\mu^2}{E^2} \right) \\ &= \frac{4\pi\alpha^2}{3s} \sqrt{1 - \frac{4m_\mu^2}{s}} \left( 1 + \frac{2m_\mu^2}{s} \right). \end{aligned}$$

We can now plug in numbers to get the cross section and number of expected events for different energies for a given luminosity and detection efficiency. The results are shown in fig. (1).

$\sqrt{s}$ [GeV]	$\sigma(\sqrt{s})$ [pb]	Events
5	3474.36	86859
50	34.74	868
91	10.49	262
125	5.56	139

Figure 1: Table showing cross sections and expected number of events at different energies when the luminosity is  $100\text{pb}^{-1}$  and detection efficiency is 50%.

### 1.3 Electroweak calculation

In order to calculate the cross section for muon pair production for high energies we must take into account the Z. Thus we get two feynman diagrams, one with  $\gamma$  and one with Z, which gives us four terms to calculate when we square the amplitude. The amplitude for the diagram involving a photon must be the same as for QED, so we can start by calculating the amplitude for the diagram with Z. Detailed calculations may be found in appendix A. The Z amplitude is

$$i\mathcal{M}_Z = \bar{v}^{t'}(p') \left( \frac{-ig_Z}{2} \gamma^\rho (C_V^e - C_A^e \gamma^5) \right) u^t(p) \left( \frac{-ig_{\rho\sigma}}{q^2 - m_Z^2} \right) \bar{u}^l(k) \left( \frac{-ig_Z}{2} \gamma^\sigma (C_V^e - C_A^e \gamma^5) \right) v^{l'}(k'),$$

where we have

$$\begin{aligned} g_Z &= \frac{e}{\sin \theta_W \cos \theta_W} \\ C_V^e &= -\frac{1}{2} + 2 \sin^2 \theta_W \\ C_A^e &= -\frac{1}{2}. \end{aligned}$$

The terms  $C_A^e$  and  $C_V^e$  is due to the fact that the weak interactions couples differently to different fermions, so the values above are those for left handed electrons and muons. We will calculate the cross section for an unpolarized  $e^+e^-$  beam, so we don't need to take the differences between left and right handed leptons into account.

The squared amplitude is then,

$$|\mathcal{M}_Z|^2 = \frac{g_Z^4}{16(q^2 - m_Z^2)^2} \left( \bar{v}^{t'}(p') \gamma^\rho (C_V^e - C_A^e \gamma^5) u^t(p) \bar{u}^t(p) \gamma^\lambda (C_V^e - C_A^e \gamma^5) v^{t'}(p') \right) \\ \left( \bar{u}^l(k) \gamma_\rho (C_V^e - C_A^e \gamma^5) v^{l'}(k') \bar{v}^{l'}(k') \gamma_\lambda (C_V^e - C_A^e \gamma^5) u^l(k) \right),$$

we can now do the same procedure with taking the trace of the two parentheses and using trace identities to get,

$$\begin{aligned} \frac{1}{4} \sum_{s,s',r,r'} |\mathcal{M}_Z|^2 &= \frac{g_Z^4}{2(q^2 - m_Z^2)^2} \left( (C_A^e{}^4 + C_V^e{}^4 + 4C_A^e{}^2 C_V^e{}^2) (p' \cdot k)(p \cdot k') \right. \\ &\quad \left. + (C_A^e{}^4 + C_V^e{}^4 - 4C_A^e{}^2 C_V^e{}^2) (p \cdot k)(p' \cdot k') \right). \end{aligned}$$

Similarly we get the cross terms by calculating,

$$\begin{aligned} |\mathcal{M}_Z \mathcal{M}_\gamma^*| &= \frac{g_Z^2 e^2}{4q^2(q^2 - m_Z^2)} \bar{v}^{t'}(p') \gamma^\rho (C_V^e - C_A^e \gamma^5) u^t(p) \bar{u}^t(p) \gamma^\mu v^{t'}(p') \\ &\quad \bar{u}^l(k) \gamma^\sigma (C_V^e - C_A^e \gamma^5) v^{l'}(k') \bar{v}^{l'}(k') \gamma^\nu u^l(k), \end{aligned}$$

which after some work takes the form,

$$\frac{1}{4} \sum_{s,s',r,r'} |\mathcal{M}_Z \mathcal{M}_\gamma^*| = \frac{2g_Z^2 e^2}{q^2(q^2 - m_Z^2)} \left( (p' \cdot k)(p \cdot k')(C_V^e{}^2 + C_A^e{}^2) + (p' \cdot k')(p \cdot k)(C_V^e{}^2 - C_A^e{}^2) \right),$$

, and finally,

$$\frac{1}{4} \sum_{s,s',r,r'} |\mathcal{M}_\gamma \mathcal{M}_Z^*| = \frac{2g_Z^2 e^2}{q^2(q^2 - m_Z^2)} \left( (p' \cdot k)(p \cdot k')(C_V^e{}^2 + C_A^e{}^2) + (p' \cdot k')(p \cdot k)(C_V^e{}^2 - C_A^e{}^2) \right),$$

thus  $|\mathcal{M}_Z \mathcal{M}_\gamma^*| = |\mathcal{M}_\gamma \mathcal{M}_Z^*|$ . We write down the total amplitude,

$$\begin{aligned} \frac{1}{4} \sum_{s,s',r,r'} |\mathcal{M}|^2 &= \frac{1}{4} \sum_{s,s',r,r'} |\mathcal{M}_Z|^2 + \frac{1}{4} \sum_{s,s',r,r'} |\mathcal{M}_\gamma|^2 + 2 \frac{1}{4} \sum_{s,s',r,r'} |\mathcal{M}_\gamma \mathcal{M}_Z^*| \\ &= \frac{g_Z^4}{2(q^2 - m_Z^2)^2} \left( (C_A^e{}^4 + C_V^e{}^4 - 2C_A^e{}^2 C_V^e{}^2) (p' \cdot k)(p \cdot k') + (C_A^e{}^4 + C_V^e{}^4 + 6C_A^e{}^2 C_V^e{}^2) (p \cdot k)(p' \cdot k') \right) \\ &\quad + \frac{8e^4}{q^4} \left( (p' \cdot k)(p \cdot k') + (p \cdot k)(p' \cdot k') \right) \\ &\quad + \frac{4g_Z^2 e^2}{q^2(q^2 - m_Z^2)} \left( (p' \cdot k)(p \cdot k')(C_V^e{}^2 + C_A^e{}^2) + (p' \cdot k')(p \cdot k)(C_V^e{}^2 - C_A^e{}^2) \right), \end{aligned}$$

where we dropped the muon mass term in the amplitude from the QED part because we'll look at high energies. The total amplitude can be simplified in the same way as we did for QED, we get,

$$\begin{aligned} \frac{1}{4} \sum_{s,s',r,r'} |\mathcal{M}|^2 &= e^4(1 + \cos^2 \theta) + \frac{g_z^4 E^4}{(s - m_Z^2)^2} \left( (1 + \cos^2 \theta)(C_V^{e2} + C_A^{e2})^2 + 8C_V^{e2}C_A^{e2} \cos \theta \right) \\ &+ \frac{8g_z^2 e^2 E^4}{s(s - m_Z^2)} \left( C_V^{e2}(1 + \cos^2 \theta) + 2C_A^{e2} \cos \theta \right). \end{aligned}$$

We plug this into the formula for the differential cross section and substitute some variables,

$$\begin{aligned} \frac{d\sigma}{d\Omega} &= \frac{\alpha^2}{4s} \left[ (1 + \cos^2 \theta) + \frac{s^2}{16(s - m_Z^2)^2 (\sin \theta_W \cos \theta_W)^4} \left( (1 + \cos^2 \theta)(C_V^{e2} + C_A^{e2})^2 + 8C_V^{e2}C_A^{e2} \cos \theta \right) \right. \\ &\quad \left. + \frac{s}{2(s - m_Z^2)(\sin \theta_W \cos \theta_W)^2} \left( C_V^{e2}(1 + \cos^2 \theta) + 2C_A^{e2} \cos \theta \right) \right] \quad (4) \end{aligned}$$

This expression we can integrate over  $d\Omega$  and get,

$$\sigma_{\text{CM}} = \frac{4\pi\alpha^2}{3s} \left( 1 + \frac{s^2}{16(s - m_Z^2)^2 (\sin \theta_W \cos \theta_W)^4} (C_V^{e2} + C_A^{e2})^2 + \frac{s}{2(s - m_Z^2)(\sin \theta_W \cos \theta_W)^2} C_V^{e2} \right)$$

## 1.4 Results

In fig. (2) we have the QED analytical cross section. The form of the analytical expression is very simple and shows us a decreasing cross section when then center of mass energy increases. For the electroweak case we have a more complicated expression, when looking at it we expect the cross section to decrease for higher energies and have a peak at  $s = m_Z^2$ , and this is what we see in fig. (3).

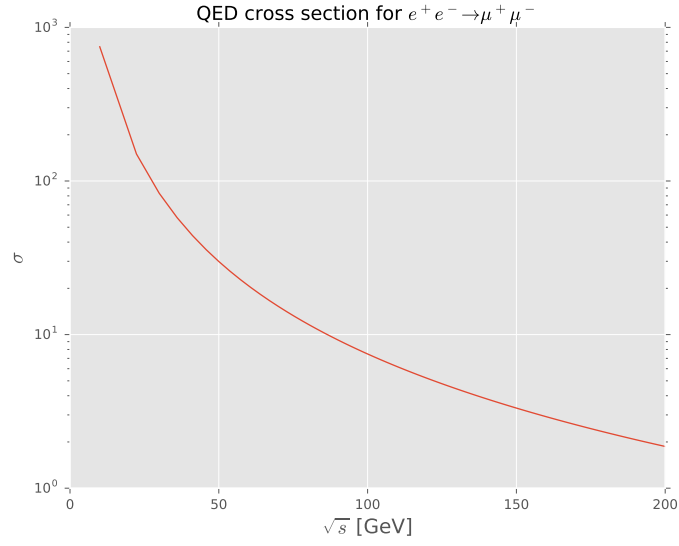


Figure 2: *Analytical QED cross section for muon pair production. The cross section decreases for higher energies.*

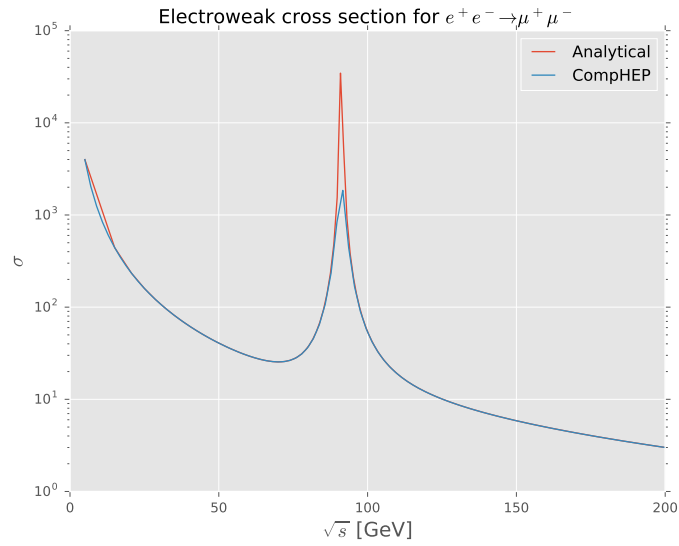


Figure 3: *Analytical and numerical electroweak cross section for muon pair production. The cross section decreases for higher energies and has a peak at the Z mass. If we plot the analytical result with higher resolution the peak will be very large and the plot not so nice. The low resolution gives us the straight section at the start of the analytical graph.*

When we compare the analytical result with the numerical result we see

that they are very close to each other. However, if we increase the number of datapoints when plotting the analytical solution we'll get a enormous Z peak since we don't have a way to handle the singularity when  $s = m_Z$  in a nice way in our calculation. This we see in fig. (4) at 91GeV, the analytical cross section is much larger than what CompHEP predicts. This can be taken care of with some more mathematics.

$\sqrt{s}$ [GeV]	Analytical $\sigma(\sqrt{s})$ [pb]	Numerical $\sigma(\sqrt{s})$ [pb]
5	3988.4	3988.14
50	40.74	40.73
91	86208.1	2056.1
125	10.08	10.08

Figure 4: Table showing analytical and numerical cross sections for some chosen energies. The agreement between the two calculations are good, however, at 91GeV there is a large discrepancy. This may be due to some cut offs in CompHEP that we didn't do in our calculations.

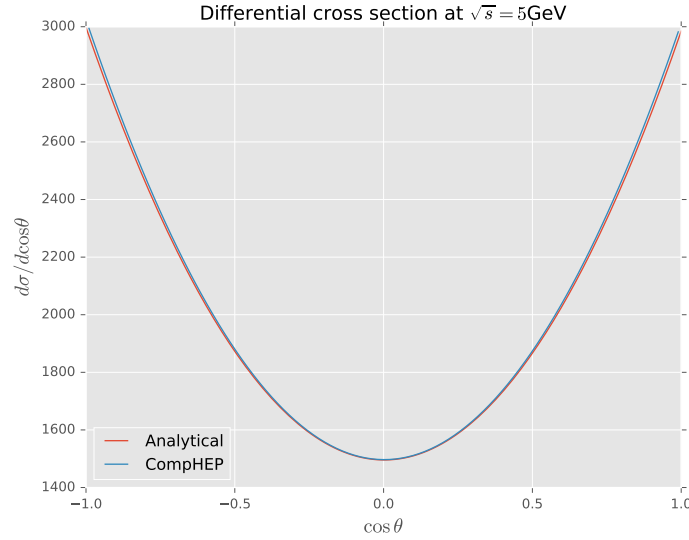


Figure 5: Here we see the differential cross section at 5GeV. From this we can expect muons coming out at all angles, but a bit less often when  $\theta = \pi/2$ , there the cross section is smaller with a factor 2 when compared to the cross section at small angles. In fig. (8) we see the angular asymmetry plotted. The difference between numerical and analytical calculations are largest at the small angles for a reason I don't yet know.



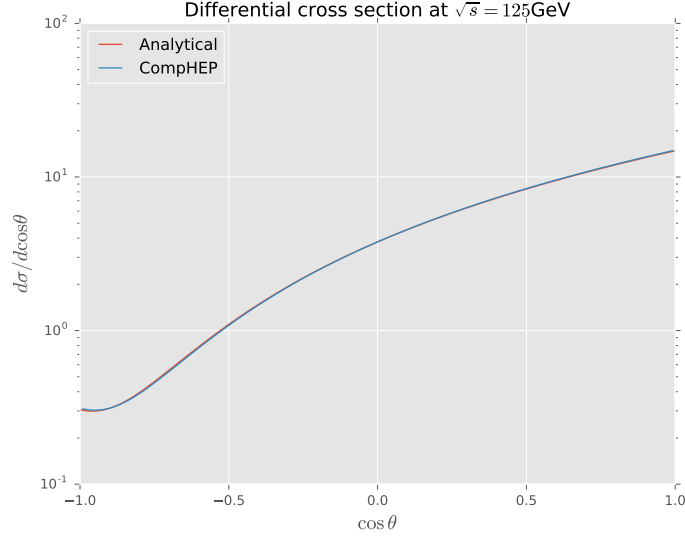


Figure 6: At 125 GeV the differential cross section is quite different from the one at 5 GeV, we see clearly that there is a difference between small angles forward and backward. For small angles forward ( $\cos \theta < 1$ ), we expect fewer particles than backward, which is quite strange! The explanation must be the behavior of the Z, since the photon doesn't care about angles. The angular asymmetry for the differential cross section is plotted in fig. (9).

Now we can take a look at the forward-backward asymmetry, to find an analytical expression for that we integrate the differential cross section twice such that we get two expressions, one for muons going forward and one for muons going backwards. That is, integrating from 0 to  $\pi/2$  and  $\pi/2$  to  $\pi$ , which results in,

$$\begin{aligned}\sigma_F(\sqrt{s}) &= \frac{2\pi\alpha^2}{3s} \left( 1 + \frac{s^2}{16(s - m_Z^2)^2 (\cos \theta_W \sin \theta_W)^4} ((C_V^{e2} + C_A^{e2})^2 + \frac{1}{3} C_V^{e2} C_A^{e2}) \right. \\ &\quad \left. + \frac{s}{2(s - m_Z^2) (\cos \theta_W \sin \theta_W)^2} (C_V^{e2} + \frac{3}{4} C_A^{e2}) \right) \\ \sigma_B(\sqrt{s}) &= \frac{2\pi\alpha^2}{3s} \left( 1 + \frac{s^2}{16(s - m_Z^2)^2 (\cos \theta_W \sin \theta_W)^4} ((C_V^{e2} + C_A^{e2})^2 - \frac{1}{3} C_V^{e2} C_A^{e2}) \right. \\ &\quad \left. + \frac{s}{2(s - m_Z^2) (\cos \theta_W \sin \theta_W)^2} (C_V^{e2} - \frac{3}{4} C_A^{e2}) \right).\end{aligned}$$

Then we can plot the asymmetry as,

$$A_{FB}(\sqrt{s}) = \frac{\sigma_F(\sqrt{s}) - \sigma_B(\sqrt{s})}{\sigma_F(\sqrt{s}) + \sigma_B(\sqrt{s})},$$

which gives us fig. (7).

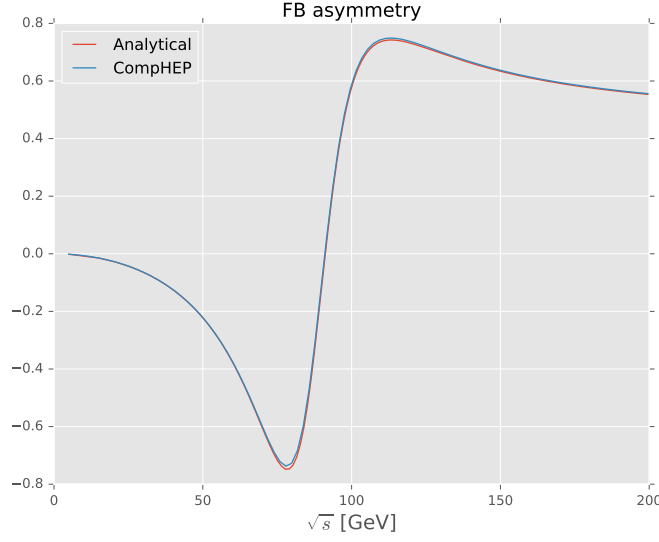


Figure 7: Analytical and numerical calculation of forward-backward asymmetry, these results are in good agreement. This plot shows in which direction the particles will go at different energies, e.g. at low energies we expect most of the particles to go forwards ( $\theta > \pi/2$ ), while at high energies most of them will go backwards ( $\theta < \pi/2$ ).

When looking at fig. (7), we expect the ratio of particles going forward compared to the number of those going backward to change when the center of mass energy increases. For *low* energies the asymmetry is small, but gets larger when closer to the Z peak. Before the peak we expect most particles forward,  $\theta > \pi/2$  where  $\theta$  is the angle between the incoming momentum and outwards momentum, and after the peak we expect most particles to go *backwards*. Finally, we want to look at the asymmetry for the differential cross section, this we do by integrating eq. (4) over  $\phi$  and inserting  $\cos \theta_F = [1, 0]$  and  $\cos \theta_B = [0, -1]$  to get,

$$A_{FB}(\cos \theta) = \frac{\frac{d\sigma_F}{d\cos \theta} - \frac{d\sigma_B}{d\cos \theta}}{\frac{d\sigma_F}{d\cos \theta} + \frac{d\sigma_B}{d\cos \theta}}. \quad (5)$$

Plotting eq. (5) gives us the results in fig. (8), (9), and (10).

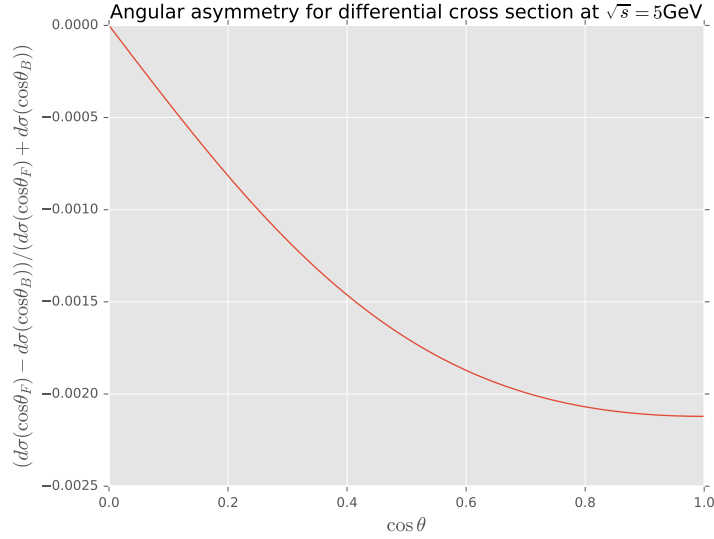


Figure 8: When looking at fig. (5) we expect this plot to show that the outgoing muons will move circa equal backward and forward, which we indeed see here. The difference between particles going forward and backward are rather small.

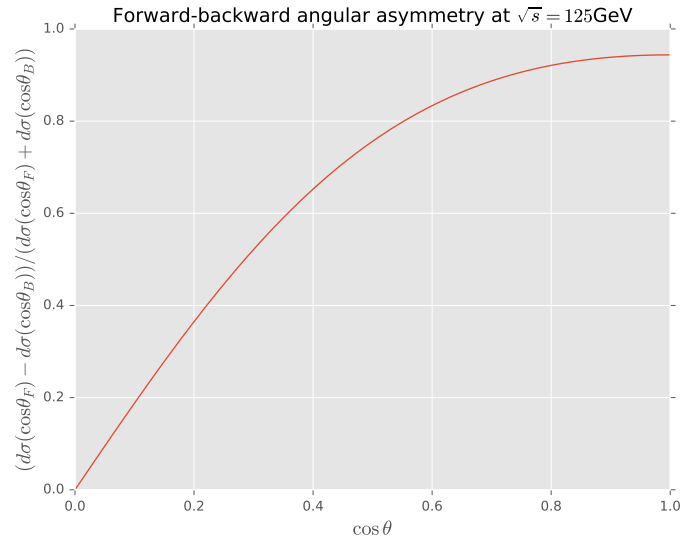


Figure 9: Angular asymmetry at 125 GeV. When looking at fig. (7) we expect this plot to show that the particles will move backwards, so this seems fine. Almost zero particles will go forward compared to the number of particles going backwards.

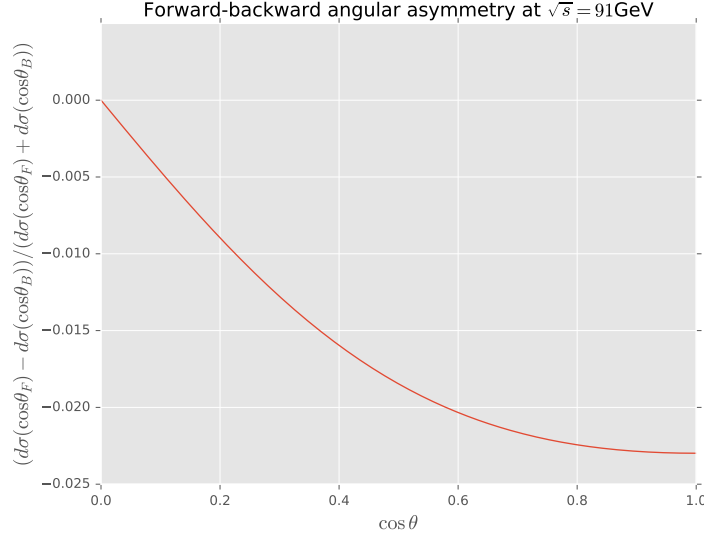


Figure 10: Angular asymmetry at 90GeV. When looking at fig. (7) we expect this plot to show that the particles will move circa equally forward and backwards. If we plot at energies closer to the Z mass we'll get a line that is even closer to zero, but at the Z mass the numerical calculation will break down due to the singularity in the analytical differential cross section expression.

From these calculations we now know the cross section for muon pair production at different energies and how the particles will be angularly distributed in the detector. This can be used to confirm that we indeed have a Z boson.

## 2 Di-lepton production beyond SM

### 2.1 Motivation for Z'

The electroweak model's W boson couples only to lefthanded fermions, this indicate that some symmetry is broken, namely parity. By introducing a right handed group to the electroweak theory,  $SU(2)_R$ , we will have a symmetry between left and right and this gives us some new vector bosons,  $W^{\pm'}$  and  $Z'$ . The new  $W'$  will only couple to right handed fields, while the  $Z'$  will behave just like the Z we already know. However, there are several ways to construct these theories, and an experimental discovery will tell us how a GUT should look like.

If we introduce the  $Z'$  with exactly the same interactions as the Z we get the same processes as in (1) and (2), and also a  $q\bar{q}$  pair instead of  $e^+e^-$  is possible.

### 2.2 Current limits

Different models predict different  $Z'$ -masses, an Atlas paper [1] from 2016 says that the limits varies from 2.74TeV to 3.36TeV.

In fig. (11) and (12) we see the cross section and asymmetry for energies up to

2TeV after a  $Z'$  boson is added to our model. The  $Z'$  mass is set to be 1TeV. We see that we will get the same peak as for the known  $Z$ , just at higher energy. This is not surprising since we added a particle with the same interactions as  $Z$  only with a higher mass.

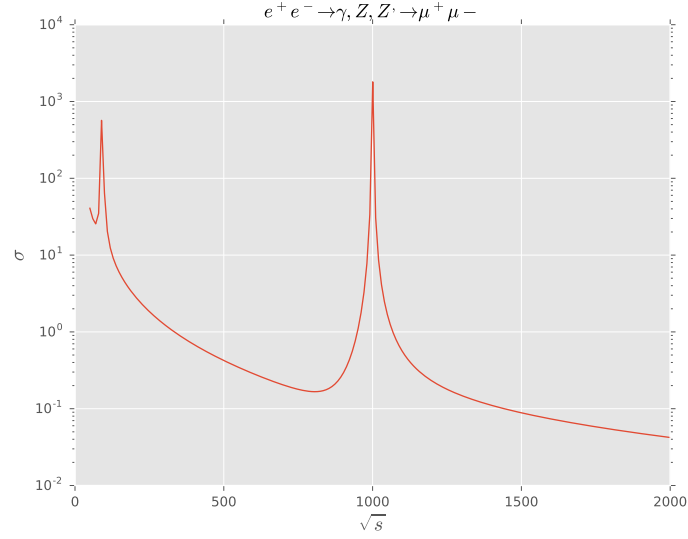


Figure 11: Cross section as function of COM energy in GeV. When adding a  $Z'$  we get a new peak at the new boson's mass which is similar to that of  $Z$ .

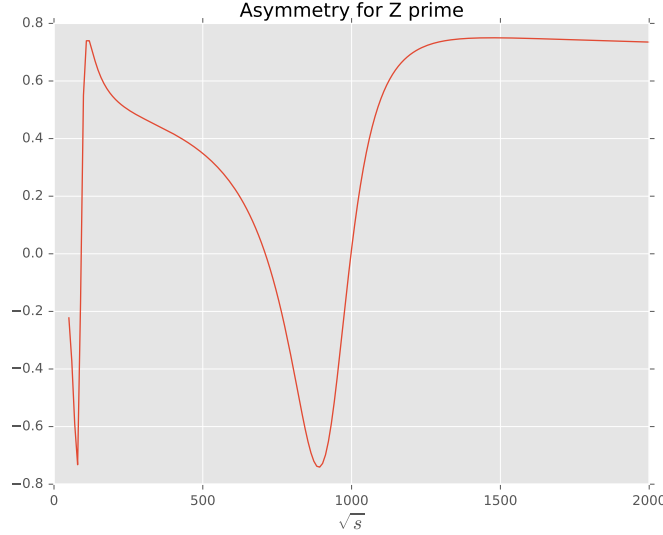


Figure 12: *The forward-backward asymmetry plotted as function of COM energy in GeV. As we can expect, the same pattern repeats when adding a new vector boson with higher mass.*

From before we know the expression for invariant mass which we calculate from the momentum of the outgoing particles,

$$m^2 = (|p_1| + |p_2|)^2 - (p_1 + p_2)^2.$$

However, it is hard to reconstruct the invariant mass, the transverse mass is introduced. It is a concept that is quite similar, but now we use the transverse momentum to calculate the mass,

$$m_T^2 = (|p_{1,T}| + |p_{2,T}|)^2 - (p_{1,T} + p_{2,T})^2.$$

In addition to that it is possible to find the transverse mass, it is also easy to measure the  $W$  mass very precisely with this method. In [2] we're introduced to the other way of writing this,

$$m_T = \sqrt{2p_{1,T}p_{2,T}(1 - \cos \Delta\phi_{p_{1,T}p_{2,T}})}, \quad (6)$$

where  $\Delta\phi_{p_{1,T}p_{2,T}}$  is the angle between the outgoing (for example) lepton momentum and the missing transverse momentum (which we find from looking at all products from the reaction, not only what the produced  $W$  decays into). If we think of  $p_{2,T}$  as the transverse momentum to a neutrino (which is likely to get from a  $W$  decay), it will be the same as the missing transverse momentum since we're not able to measure the neutrinos.

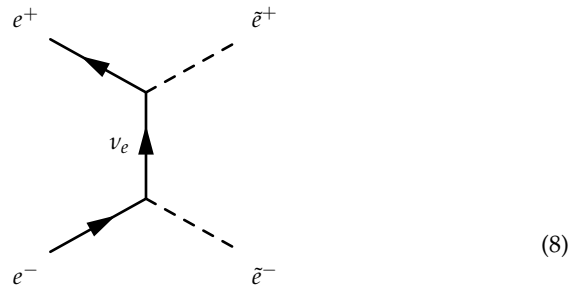
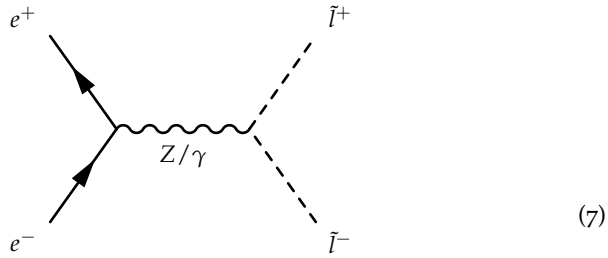
As mentioned above,  $Z'$  is produced by the same reactions as  $Z$  since it has all the same couplings. The  $W'$  are produced in the same way as  $W$ , but now with right handed fermions. Since the new bosons are produced much the same way as the already known bosons, we will have much background from the known bosons.

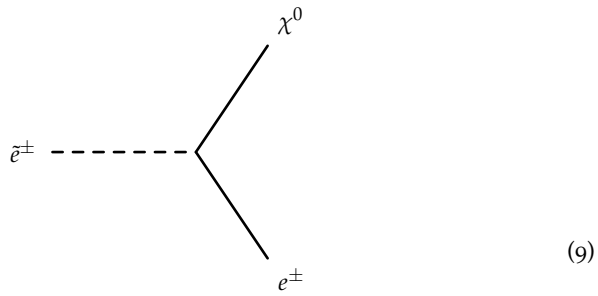
Signs of  $Z'$  will be visible as a peak at its mass. For  $W'$  we can use the transverse mass, (6). We can look at the distribution of transverse momentum, this will increase up to half the mass of  $W'$  before it suddenly goes to zero, this is called a *Jacobian peak*. The reason for this large drop is because all transverse momentum comes from the decay of the  $W$ , and we can't have more transverse momentum than the mass of the  $W$ . Thus, we'll barely have events where a lepton and a neutrino have transverse momentum larger than the  $W$  mass. The same method can be used to find the  $W'$ .

### 2.3 Slepton pair production

As shown in diagram (7) a slepton pair can be produced from a  $Z$  or  $\gamma$ . Another possibility is (8) with a neutrino. The signature of this process can be found by looking at what the sleptons are most likely to decay into. According to [3] sleptons can decay into a lepton and a neutralino, see (9), it is also possible with a sneutrino and  $W$ . If we are lucky enough to produce the Lightest Supersymmetric Particle (LSP) we will have a signal that is two leptons and missing  $p_T$ . Unfortunately this is exactly the same signal as the double  $W$  production has, there we get two leptons and two anti neutrinos which fly away with the missing  $p_T$ .

So, how do we separate signal and background? No one knows! The *transverse mass* is inspired by the transverse mass and is a function of two visible particles momenta and the missing transverse momentum in an event. This can be used in events like those we are looking at now.





## References

- [1] Morad Aaboud et al. Search for high-mass new phenomena in the dilepton final state using proton-proton collisions at  $\sqrt{s} = 13$  TeV with the ATLAS detector. *Phys. Lett.*, B761:372–392, 2016.
- [2] Magnar K. Bugge. Observation of heavy gauge bosons decaying to lepton-neutrino pairs - the SM W boson and new, heavy W' bosons (?). 2011. <http://folk.uio.no/farido/FYS4560-Magnar-W'.pdf>.
- [3] Stephen P. Martin. A Supersymmetry primer. 1997. [Adv. Ser. Direct. High Energy Phys.18,1(1998)].